

# Stress response and nutrient homeostasis in lettuce (*Lactuca sativa*) exposed to graphene quantum dots are modulated by particle surface functionalization

Zhang, Peng; Wu, Xinyue; Guo, Zhiling; Yang, Xiaonan; Hu, Xiangang; Lynch, Iseult

DOI:

[10.1002/adbi.202000778](https://doi.org/10.1002/adbi.202000778)

License:

Creative Commons: Attribution (CC BY)

*Document Version*

Publisher's PDF, also known as Version of record

*Citation for published version (Harvard):*

Zhang, P, Wu, X, Guo, Z, Yang, X, Hu, X & Lynch, I 2021, 'Stress response and nutrient homeostasis in lettuce (*Lactuca sativa*) exposed to graphene quantum dots are modulated by particle surface functionalization', *Advanced Biology*, vol. 5, no. 4, 2000778, pp. 2000778. <https://doi.org/10.1002/adbi.202000778>

[Link to publication on Research at Birmingham portal](#)

## General rights

Unless a licence is specified above, all rights (including copyright and moral rights) in this document are retained by the authors and/or the copyright holders. The express permission of the copyright holder must be obtained for any use of this material other than for purposes permitted by law.

- Users may freely distribute the URL that is used to identify this publication.
- Users may download and/or print one copy of the publication from the University of Birmingham research portal for the purpose of private study or non-commercial research.
- User may use extracts from the document in line with the concept of 'fair dealing' under the Copyright, Designs and Patents Act 1988 (?)
- Users may not further distribute the material nor use it for the purposes of commercial gain.

Where a licence is displayed above, please note the terms and conditions of the licence govern your use of this document.

When citing, please reference the published version.

## Take down policy

While the University of Birmingham exercises care and attention in making items available there are rare occasions when an item has been uploaded in error or has been deemed to be commercially or otherwise sensitive.

If you believe that this is the case for this document, please contact [UBIRA@lists.bham.ac.uk](mailto:UBIRA@lists.bham.ac.uk) providing details and we will remove access to the work immediately and investigate.

# Stress Response and Nutrient Homeostasis in Lettuce (*Lactuca sativa*) Exposed to Graphene Quantum Dots Are Modulated by Particle Surface Functionalization

Peng Zhang,\* Xinyue Wu, Zhiling Guo, Xiaonan Yang, Xiangang Hu, and Iseult Lynch

A 5-d germination assay and a 14-d hydroponic trial are performed to evaluate the impacts of graphene quantum dots (GQDs) on lettuce. Results show that GQDs are toxic to lettuce plants and that the effects are highly dependent on particle surface functionalization and plant growth stage. The germination rate is not affected by aminated GQDs (N-GQDs) and carboxylated GQDs (C-GQDs) but is reduced by hydroxylated GQDs (O-GQDs) by 39–71%. During the hydroponic trial, N-GQDs (50 mg L<sup>-1</sup>) increase the root dry weight by 34%, while C-GQDs and O-GQDs reduce it by 39% and 43%, respectively. Shoot dry weight is not affected by N-GQDs but is reduced by C-GQDs (44%) and O-GQDs (36–55%) treatments. C-GQDs and O-GQDs cause oxidative damage, disruption of mineral and organic nutrients homeostasis, impairment of photosynthesis, and modulates the levels of phytohormones. Light-triggered reactive oxygen species generation and oxidation of antioxidants in plants are the critical reason for the phytotoxicity and explain the difference between the different functionalizations. These findings suggest that GQDs may not be as safe as expected. Future studies should consider the modulation of surface chemistry to achieve optimal safety of GQDs, and more plant species should be tested over a longer-term scale.


## 1. Introduction

Nanomaterials (NMs) have great potential for a range of applications in agriculture, to enhance crop productivity, improve

Dr. P. Zhang, X. Wu, Dr. Z. Guo, Prof. I. Lynch  
School of Geography, Earth and Environmental Science  
University of Birmingham  
Edgbaston, Birmingham B15 2TT, UK  
E-mail: p.zhang.1@bham.ac.uk

Dr. X. Yang  
School of Environment  
Harbin Institute of Technology  
73 Huanghe Road, Nangang District, Harbin 150036, China

Prof. X. Hu  
Key Laboratory of Pollution Processes and Environmental Criteria  
(Ministry of Education)  
College of Environmental Science and Engineering  
Nankai University  
Tianjin 300071, China

 The ORCID identification number(s) for the author(s) of this article can be found under <https://doi.org/10.1002/adbi.202000778>.

© 2021 The Authors. Advanced Biology published by Wiley-VCH GmbH. This is an open access article under the terms of the Creative Commons Attribution License, which permits use, distribution and reproduction in any medium, provided the original work is properly cited.

DOI: 10.1002/adbi.202000778

the soil health, improve the performance of agrochemicals, and reduce runoff-associated environmental deterioration.<sup>[1]</sup> Scientific publications related to the application of nanotechnology in agriculture have growing exponentially in the last decades. However, compared to other fields of nanotechnology application such as biomedical, water and energy, the agricultural sector is still marginal in terms of real applications with nanotechnology applications still in early stages of development.<sup>[2]</sup> Lack of fundamental understanding of the interactions of and transformations of NMs within soil and plant systems is the key barrier to move this field forward,<sup>[1a]</sup> although many efforts have been made till today to build knowledge. To achieve the desired functions from NMs in plants, such as delivery of NMs to targeted places (e.g., chloroplasts),<sup>[3]</sup> mechanistic understanding of how NMs are translocated and transformed in plants and how the phys-

icochemical properties of the NMs affect these behaviours, is imperative.

Carbon based NMs such as graphene and carbon quantum dots, have attracted immense interest in terms of their potential for agri-environmental applications, which arises is large part from the fact that they are composed of carbon, the most abundant elements on earth and the basic elements of living organisms, which is assumed to endow them with low toxicity and minimal environmental impact. Graphene has shown potential as a carrier for fertilizers to enable smart release thus enhance the nutrient use efficiency by plants.<sup>[4]</sup> The Zn or Cu nutrients loaded on graphene oxide (GO) sheets release fast (≈40%) in 5 h and in a slow and sustained way at later stages. A recent study also showed that graphene quantum dots (GQDs) can also be used as a plant growth enhancer.<sup>[5]</sup>

Graphene quantum dots (GQDs), as a zero-dimensional NM of the carbon family NMs, have attracted increasing attention due to their unique electronic properties, photoluminescence, chemical stability and biocompatibility.<sup>[6]</sup> The application of GQDs is several-fold, including as bioimaging makers, antibacterial agents, sensors, energy and electronic materials. The recent progress of nano-enabled sustainable agriculture also offers GQDs the potential for application in agricultural sector. Moreover, GQDs synthesis from natural carbon sources such as coal has opened up the possibility of their large-scale production and low cost, as

required for agricultural application. The most common applications of GQDs in the agri-environmental sector is the detection of heavy metals and organic molecules based on their luminescence and electrochemical properties. For example, GQDs have been incorporated into nylon or PVA to enable the fluorescence detection of Cr(VI) or Hg(II) with a detection limit of 190 nM for Cr(VI) and 100 nM for Hg(II).<sup>[7]</sup> Beyond that, a few recent studies showed that GQDs may directly act as a plant growth enhancer, although such studies are still limited. Seed priming with 200 mg L<sup>-1</sup> GQDs for 3 h improved the growth of coriander and garlic including the seedling, flower and fruit.<sup>[5]</sup> Xu et al. found that GQDs with a size of 10 nm and concentration of 400 mg L<sup>-1</sup> promoted the growth of *Zephyranthes grandiflora* in a size-dependent manner.<sup>[8]</sup> However, Feng et al. reported that the effect of GQDs (1.8–3.6 nm) on plant growth was dependent on the plant species;<sup>[9]</sup> GQDs inhibited the seedling elongation of mung bean when the concentration was higher than 250 mg L<sup>-1</sup> and caused 80% of reduction at 1500 mg L<sup>-1</sup>, while the GQDs showed no significant effects on tomato until up to 1250 mg L<sup>-1</sup> (38%).<sup>[9]</sup>

Thus, contradictory results regarding the impacts of GQDs in plants have been reported. Notably, these studies used unrealistically high concentrations ranging from 200 to 1500 mg L<sup>-1</sup>. Before agricultural application of GQDs can be pursued in real agricultural systems, more studies are required to fully understand the interaction of GQDs and plants at low exposure concentrations, which includes the potential adverse impacts of the GQDs on plant growth, the overall agricultural ecosystem and cumulative effects of repeated application of GQDs. A key aspect that is currently poorly understood is the influence of GQDs

physicochemical properties (e.g., size, height, surface chemistry) on their transformation processes and interaction with plants.

The aim of this study is to investigate the impacts of GQDs on plant growth across a range of low concentrations and explore how surface functionalization of the GQDs influences their effects on plants. We used head lettuce as a model plant species, as it is a widely consumed leaf vegetable worldwide. Impacts of O-GQDs, C-GQDs, and N-GQDs with different surface functionalizations on lettuce growth were compared. A 5-d germination assay was performed with the seed germination, root elongation, cell death and oxidative stress being evaluated. In a hydroponic trial, impacts of GQDs on plant biomass, photosynthetic system, mineral nutrient homeostasis, organic nutrient content, antioxidant enzyme system and phytohormone levels were evaluated. The intrinsic reactive oxygen species (ROS) generation and oxidative potential of GQDs were investigated to understand the difference in the phytotoxicity modulated by the particle surface functionalization.

## 2. Results

### 2.1. Characterization of the GQDs

The sizes obtained from the TEM images (Figure 1A) were  $5.3 \pm 0.8$ ,  $8.1 \pm 1.3$  and  $6.4 \pm 0.7$  nm for N-GQDs, C-GQDs and O-GQDs, respectively. 3D EEMs images (Figure 1B) showed well-defined luminescent regions for all the GQDs, with the maximum peak in the blue region ( $E_x/E_m = 250\text{--}275/320\text{--}420$  nm). FTIR

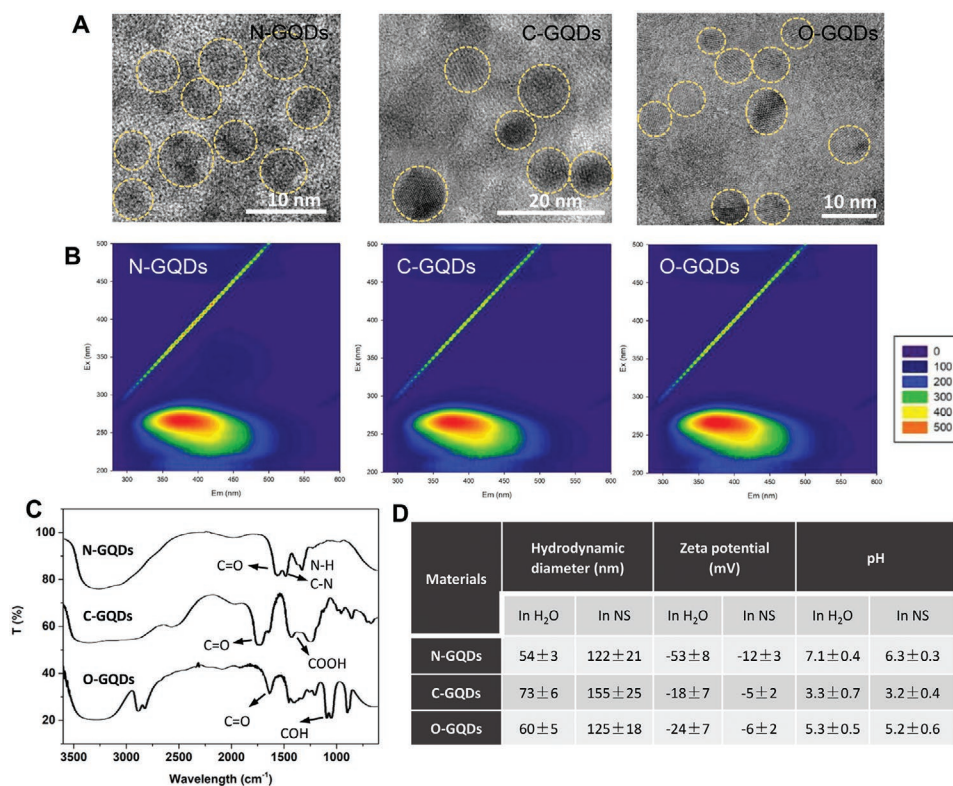


**Figure 1.** A) TEM images, B) 3D EEM images, C) FTIR spectra, and D) summary of hydrodynamic size, zeta potential and pH of GQDs. NS indicates nutrient solution.

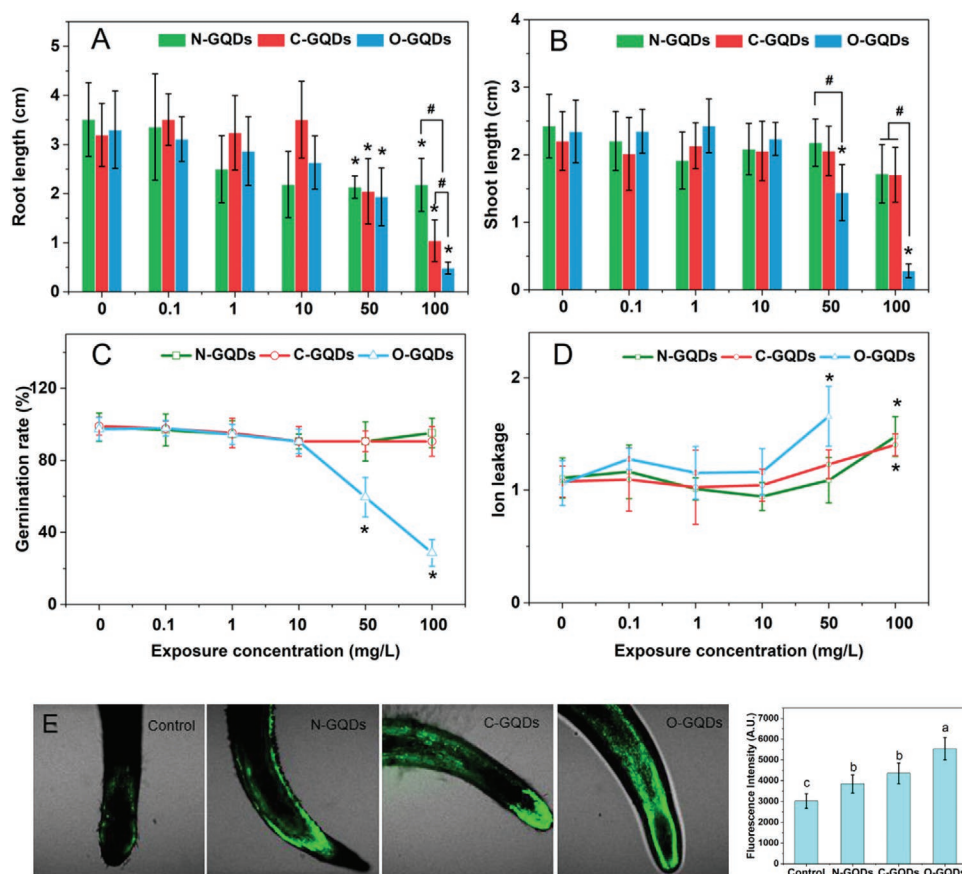


**Figure 2.** Impact of GQDs on A) root and B) shoot elongation, C) seed germination, D) cell membrane integrity measured by ion leakage during the seed germination stage, and E) ROS accumulation in the roots after 5 days of exposure to GQDs ( $50 \text{ mg L}^{-1}$ ). At least ten images were taken for each treatment. \* indicates significant difference at  $p < 0.05$  ( $n = 6$ ) compared with control. Different lowercase letters indicate significant difference at  $p < 0.05$  ( $n = 6$ ) compared between treatments evaluated by one way ANOVA analysis.

spectra (Figure 1C) showed clearly the presence of N-H/C-N in N-GQDs ( $1498 \text{ cm}^{-1}$ ), COOH in C-GQDs ( $1400 \text{ cm}^{-1}$ ), and C-OH in O-GQDs ( $1098 \text{ cm}^{-1}$ ). The average hydrodynamic sizes of N-GQDs, C-GQDs, and O-GQDs in deionized water were 54, 73, and 60 nm, respectively. Larger aggregates formed in the nutrient solution (NS) due to the presence of salts which contributed to the compression of the double electric layer on the particle surface and lower surface charge, which was shown by the zeta potential (Figure 1D). The lower surface charge led to weak interparticle electrostatic repulsion and ultimately particle agglomeration. Different surface functionalization resulted in distinct changes to the pH of the GQDs suspensions in water and NS, with the N-GQDs being near neutral (7.1 and 6.3 in  $\text{H}_2\text{O}$  and NS) while C-GQDs (3.3 and 3.2) and O-GQDs (5.3 and 5.2) were acidic.

## 2.2. Effects of GQDs on Seed Germination

As shown in Figure 2, none of the three GQDs showed any significant impact on seed germination including root and shoot elongation or on the germination rate until  $10 \text{ mg L}^{-1}$ . The three GQDs reduced the root elongation to similar extents (by 40%, 36%, and 41%) at  $50 \text{ mg L}^{-1}$  (Figure 2A). When the concentration increased to  $100 \text{ mg L}^{-1}$ , the GQDs showed significantly

different effects on root elongation, with the highest reduction being observed for O-GQDs (85%) followed by C-GQDs (41%) and then N-GQDs (32%). The shoot elongation was affected only by O-GQDs, with reduction of 39% and 88% at 50 and  $100 \text{ mg L}^{-1}$ , respectively (Figure 2B). The germination rate was not affected by N-GQDs and C-GQDs but was reduced by O-GQDs by 39% and 71% at 50 and  $100 \text{ mg L}^{-1}$ , respectively (Figure 2C). The membrane integrity of root cells was evaluated by measuring the ion leakage (Figure 2D). C-GQDs and N-GQDs at  $100 \text{ mg L}^{-1}$  caused similar extents of increase of ion leakage, which were 30% and 33%, respectively. More severe cell damage was caused by the O-GQDs, with 56% increase of ion leakage observed at  $50 \text{ mg L}^{-1}$ . Data at  $100 \text{ mg L}^{-1}$  was not tested for O-GQDs because the root germination was almost halted. Over accumulation of ROS in plant roots was observed for all GQDs ( $50 \text{ mg L}^{-1}$ ), with the highest for O-GQDs.

## 2.3. Effects of GQDs on Biomass Production of Lettuce at Seedling Stage

The impacts of GQDs on the growth of lettuce at seedling stage was evaluated by measuring the biomass production (Figure 3). The root dry weight was increased by 34% after 14 days of



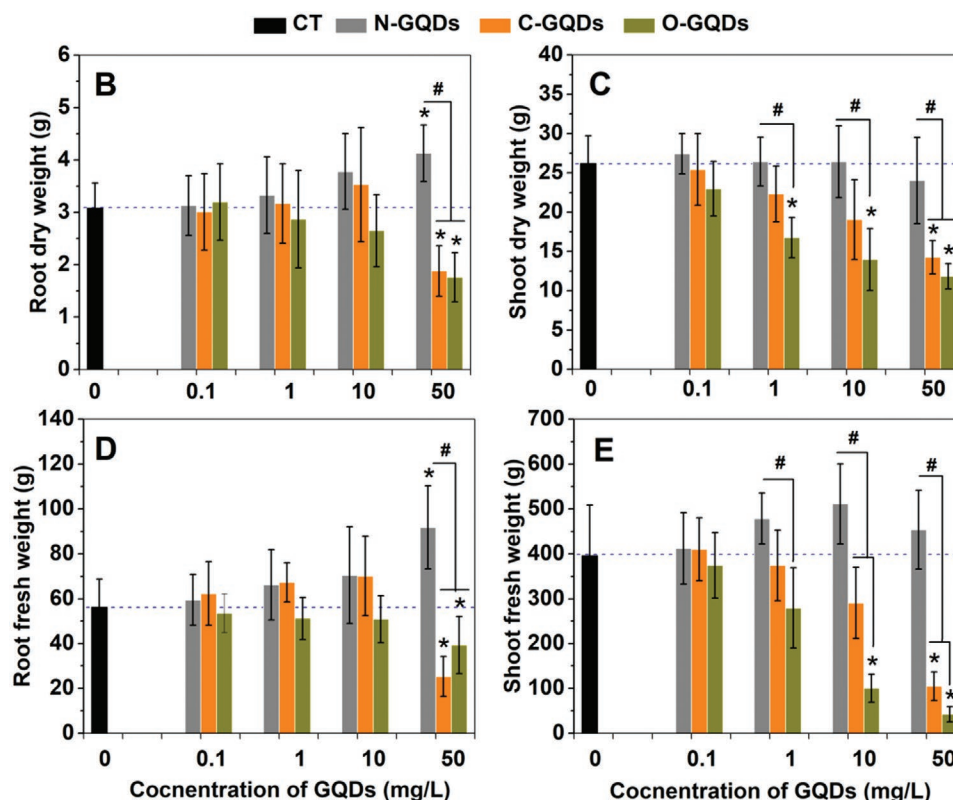


**Figure 3.** Fresh weight and dry weight of plant seedlings exposed to GQDs for 2 weeks. \* and # indicate significant difference at  $p < 0.05$  ( $n = 6$ ) compared with control and between groups, respectively, evaluated by one way ANOVA analysis.

treatment with N-GQDs ( $50 \text{ mg L}^{-1}$ ) while it was reduced by 39% and 43% with C-GQDs and O-GQDs treatments ( $50 \text{ mg L}^{-1}$ ). Shoot dry weight was not affected by N-GQDs but was reduced by 44% with  $50 \text{ mg L}^{-1}$  C-GQDs treatment and by 36%, 47%, and 55%, respectively, with 1, 10 and  $50 \text{ mg L}^{-1}$  O-GQDs treatment. A similar trend of impact was observed for lettuce fresh weight. N-GQDs of  $50 \text{ mg L}^{-1}$  increased the fresh weight of root by 63% while C-GQDs and O-GQDs reduced the root fresh weight by 55% and 31%, respectively. The shoot fresh weight was reduced by 74% following  $10 \text{ mg L}^{-1}$  O-GQDs treatment and by 74% and 89%, respectively, with  $50 \text{ mg L}^{-1}$  C-GQDs and O-GQDs treatment.

#### 2.4. Effects of GQDs on Photosynthetic System

Leaf moisture as a key component to support photosynthesis was evaluated by calculating the weight loss after drying of the fresh samples (Figure 4A). N-GQDs showed no significant effects on the leaf moisture. In contrast, C-GQDs at  $50 \text{ mg L}^{-1}$  reduced the leaf moisture by 75%. O-GQDs reduced the leaf moisture by 76% and 90% at 10 and  $50 \text{ mg L}^{-1}$ , respectively. Based on the phenotypic data, we chose 1 and  $50 \text{ mg L}^{-1}$  as the concentrations for all the following studies. N-GQDs and C-GQDs did not significantly affect the contents of the photosynthesis pigments. However,  $50 \text{ mg L}^{-1}$  of O-GQDs reduced the contents of all the pigments in the leaves, which can be visually seen from the photo of the shoots (Figure 4B). The

extent of reduction of the photosynthesis pigments by  $50 \text{ mg L}^{-1}$  O-GQDs were 65%, 60%, and 59% for Cha, Chb and carotenoids (Figure 4C,D), respectively.

#### 2.5. Alteration of Mineral Nutrient Homeostasis

Figure 5 shows the heatmap of the change of the mineral nutrient content in plant roots and leaves. GQDs at low concentrations ( $1 \text{ mg L}^{-1}$ ) did not have significant effects on the homeostasis of the minerals in roots with the exception of N-GQDs which enhanced the Zn content by 5.18-fold (Figure 5A). At high concentration ( $50 \text{ mg L}^{-1}$ ), N-GQDs induced an 0.23-fold reduction of K content and an 0.58-fold increase of Cu in roots, with no impacts on other minerals. In comparison, C-GQDs and O-GQDs disturbed the homeostasis of more elements, with 3 and 7 elements being affected, respectively. Specifically, both C-GQDs and O-GQDs increased the Ca but reduced the Mg and K contents. O-GQDs caused disturbance of four more elements, i.e., P, Fe, Mn and Zn; the contents of P, Mn, and Zn were reduced by 0.38-, 0.41-, and 0.53-fold, respectively, while the Fe content was increased by 2.51-fold.

The mineral homeostasis in leaves showed stronger sensitivity to GQDs exposure (Figure 5B) than that of roots. Contents of 2 (K and Zn), 4 (Fe, Mn, Cu, and Zn) and 6 (Ca, Mg, K, Mn, Cu, and Zn) minerals were affected by N-GQDs, C-GQDs and O-GQDs, respectively, even at  $1 \text{ mg L}^{-1}$  concentration. N-GQDs increased the K and Zn contents by 0.21- and 0.28-fold. C-GQDs

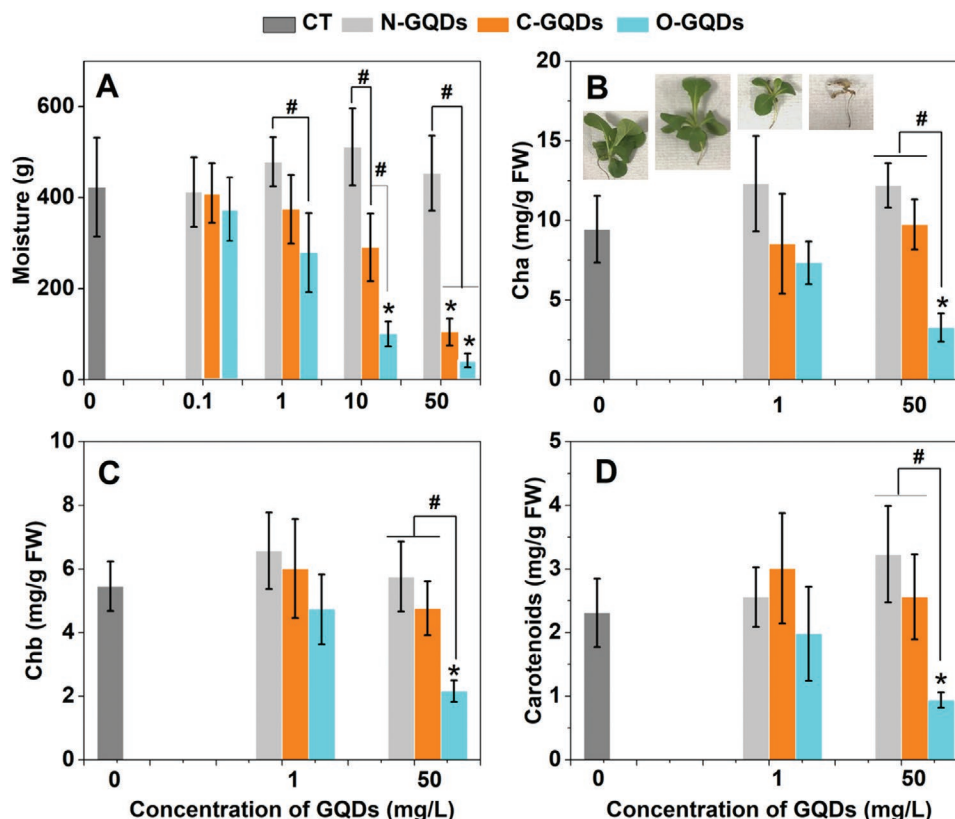


**Figure 4.** Leaf moisture (A), and the chlorophyll a (Cha) (B), chlorophyll b (Chb) (C) and carotenoid (D) contents in plant leaves after 14 days of treatment with GQDs. \* and # indicate significant difference at  $p < 0.05$  ( $n = 6$ ) compared with control and between groups, respectively, evaluated by one way ANOVA analysis.

had no impact on macro nutrients but increased the contents of all the micronutrients. O-GQDs reduced the contents of all the macronutrients (Ca, Mg, K) but increased the contents of the micronutrients (Mn, Cu, Zn). The same numbers of min-

erals were affected by 50 mg L<sup>-1</sup> GQDs as at the lower exposure concentrations. Overall, it can be seen that N-GQDs had least impact on the mineral homeostasis, followed by C-GQDs with O-GQDs causing the most effect.

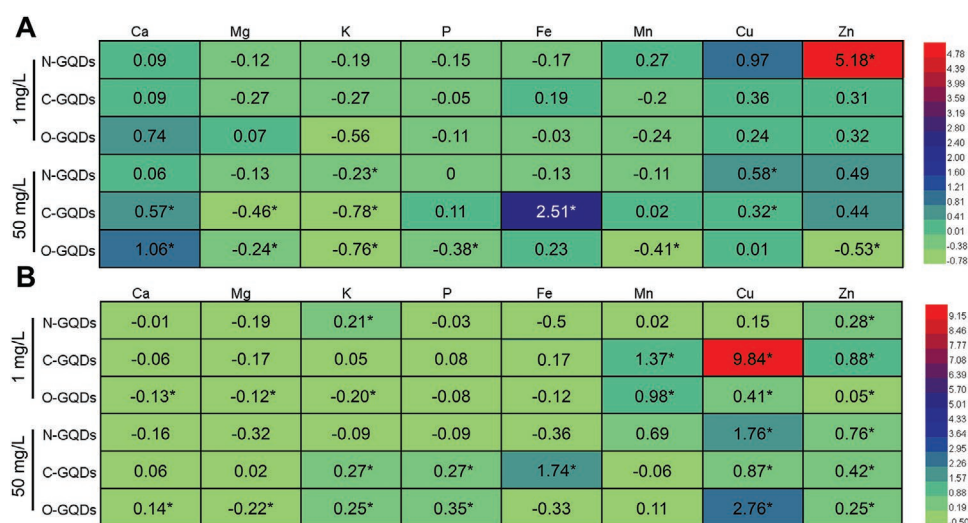


**Figure 5.** Heatmap showing the homeostasis of inorganic nutrients in root (A) and shoot (B) regulated by GQDs. Numbers indicate the fold change of elemental content compared with the control group. Minus value indicates that the content was decreased while the positive value indicates that the content was increased. \* indicates a significant difference at  $p < 0.05$  ( $n = 6$ ) compared with the control evaluated by one way ANOVA analysis.

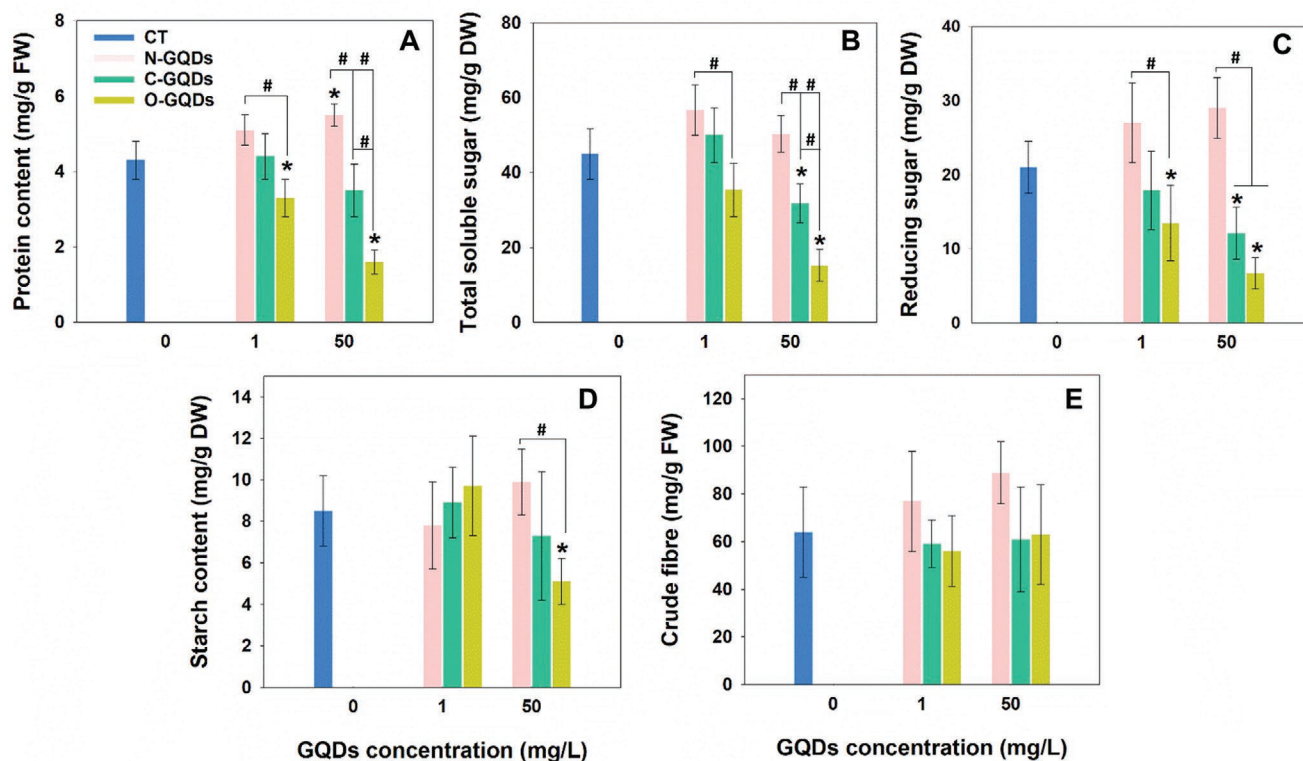


**Figure 6.** The contents of organic nutrients in lettuce leaves including total soluble protein (A), total soluble sugar (B), reducing sugar (C), starch (D), and crude fibre (E). \* and # indicate significant differences at  $p < 0.05$  ( $n = 6$ ) compared with control and between groups, respectively, evaluated by one way ANOVA analysis.

## 2.6. Organic Nutrient Accumulation

As shown in **Figure 6**, the protein content in lettuce leaves was increased by 28% with 50 mg L<sup>-1</sup> N-GQDs treatment while it was reduced by 23% and 63%, respectively, following 1 and 50 mg L<sup>-1</sup> O-GQDs treatments. The soluble sugar content was not affected by 1 mg L<sup>-1</sup> GQDs but was reduced by 29% and 66% following 50 mg L<sup>-1</sup> C-GQDs and O-GQDs treatments. Reducing sugar content was reduced by O-GQDs even at 1 mg L<sup>-1</sup>. Starch content was only affected by exposure to 50 mg L<sup>-1</sup> O-GQDs with 40% being reduced. The crude fibre content was not affected by any of the applied treatments.

## 2.7. Antioxidant Enzyme Activity and Lipid Peroxidation

As shown in **Figure 7**, in roots, SOD activities were enhanced by 38% and 33% with 1 mg L<sup>-1</sup> C-GQDs and O-GQDs treatments, respectively. However, the SOD activity was reduced by 30% following the 50 mg L<sup>-1</sup> O-GQDs treatment. POD activity was only affected by 50 mg L<sup>-1</sup> O-GQDs, with 40% being reduced. 1 mg L<sup>-1</sup> O-GQDs and 50 mg L<sup>-1</sup> C-GQDs and O-GQDs triggered 80%, 59%, and 110% increase of MDA contents in roots, suggesting cell membrane damage.

In shoots, C-GQDs at 1 mg L<sup>-1</sup> enhanced the SOD activity by 47% while they showed no effect at 50 mg L<sup>-1</sup>. O-GQDs reduced the SOD activity by 39% with no effect being observed at 1 mg L<sup>-1</sup>. C-GQDs increased the POD activity by 68% and 104% at 1

and 50 mg L<sup>-1</sup>, respectively. O-GQDs of 50 mg L<sup>-1</sup> reduced the POD activity by 51%. The MDA contents showed similar trends in shoots as in the roots. 1 mg L<sup>-1</sup> O-GQDs and 50 mg L<sup>-1</sup> C-GQDs and O-GQDs triggered 34%, 47%, and 83% increase of MDA contents in shoots, respectively. Overall, the results suggest that the antioxidant system in lettuce was triggered by the GQDs exposure. O-GQDs induced a more significant response than other two GQDs.

## 2.8. Phytohormones Contents

The impacts of GQDs on the phytohormone contents showed similar trends in roots and shoots (**Figure 8**). N-GQDs had no significant impacts on any of the tested phytohormones. The ABA contents were only affected by high concentrations of C-GQDs and O-GQDs treatments, which resulted in 84% and 154% increase in roots, and 102% and 175% increase in shoots, respectively. IAA, GA3 and ZR were exclusively reduced by C-GQDs and O-GQDs treatments. 1 mg L<sup>-1</sup> O-GQDs and 50 mg L<sup>-1</sup> C-GQDs and O-GQDs led to 34%, 36%, and 67% decrease of IAA content in roots, and 29%, 49%, and 73% decrease in shoots, respectively. 50 mg L<sup>-1</sup> C-GQDs and O-GQDs caused 43% and 65% reduction of GA3 content in roots and 36% and 67% reduction in shoots. 50 mg L<sup>-1</sup> C-GQDs and O-GQDs also caused 52% and 67% reduction of ZR content in roots and 54% and 66% reduction in shoots. O-GQDs at low concentration also caused 27% reduction of ZR in shoots. By comparing

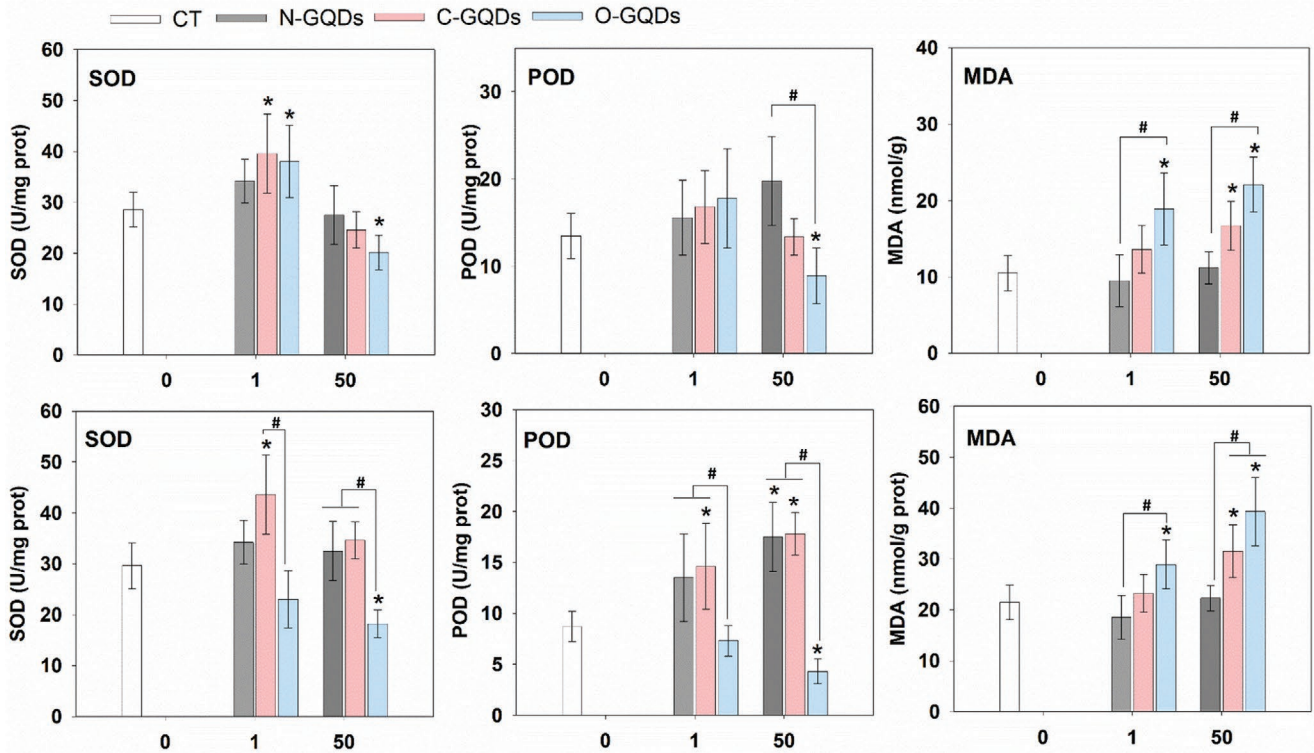


**Figure 7.** SOD and POD activities and MDA contents in roots (upper row) and shoots (bottom row) exposed to the differently surface functionalised GQDs. \* and # indicate significant differences at  $p < 0.05$  ( $n = 6$ ) compared with control and between groups, respectively, evaluated by one way ANOVA analysis.

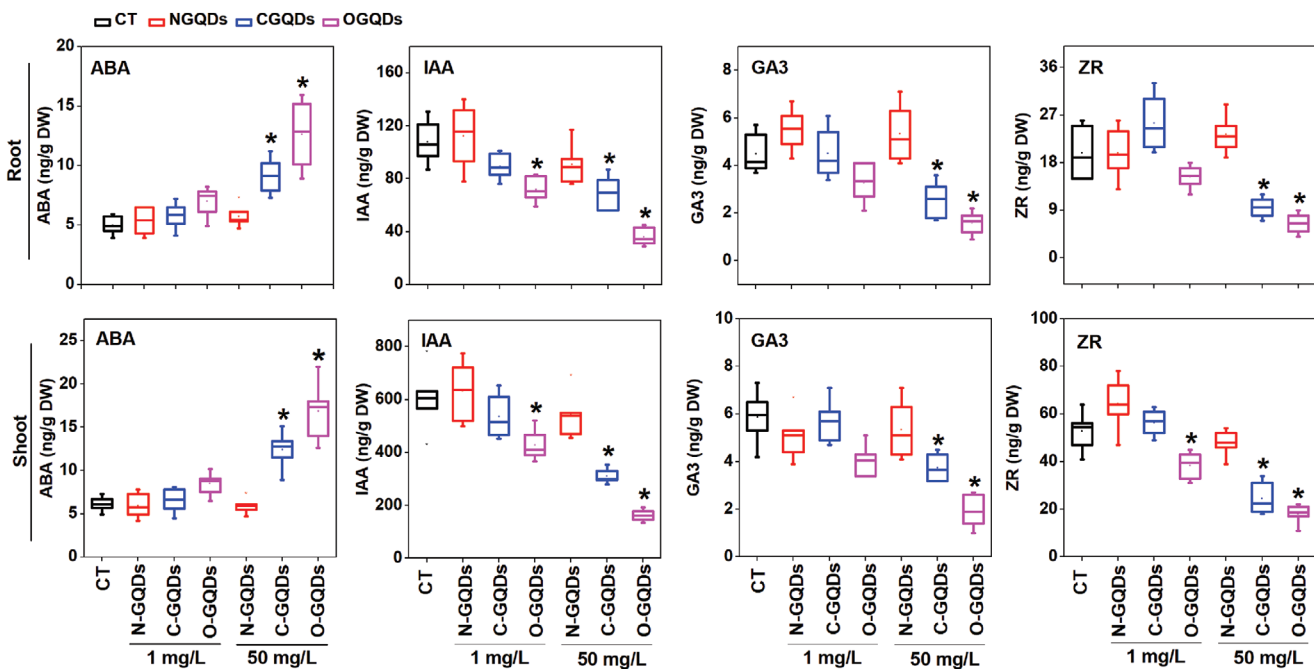


**Figure 8.** Phytohormone contents including ABA, IAA, GA3 and ZR in lettuce roots and shoots after GQDs treatments for 14 days. \* indicates significant differences at  $p < 0.05$  ( $n = 6$ ) compared with control evaluated by one way ANOVA analysis.



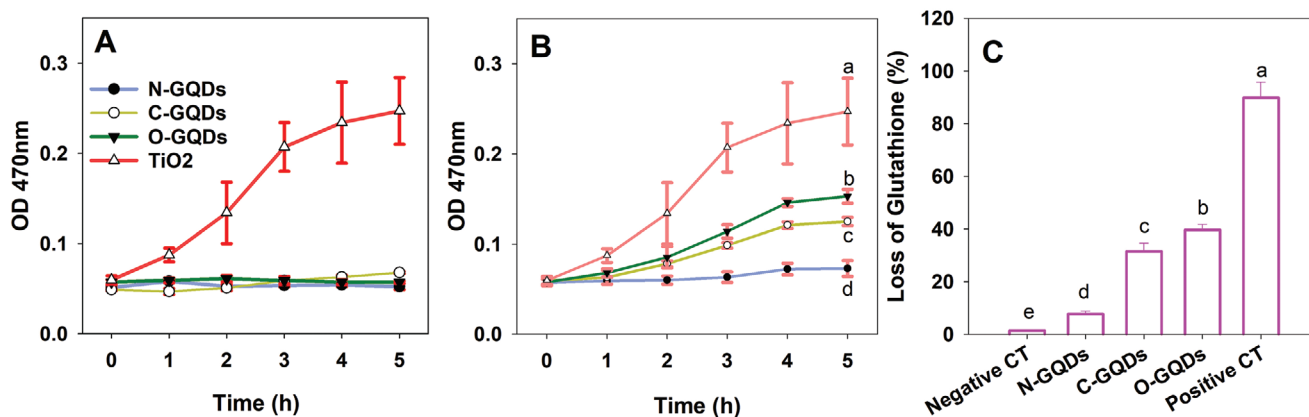


**Figure 9.** Generation of  $O_2^-$  by GQDs suspensions under dark (A) and light (B) conditions determined by the XTT test.  $TiO_2$  ( $50\text{ mg L}^{-1}$ ) under UV radiation was used as a positive control. Statistical differences between groups at 5 h were compared and expressed as lowercase letters. Different letters stand for statistical differences at  $p < 0.05$  ( $n = 6$ ) as evaluated by one way ANOVA analysis. (C) Loss of GSH after incubation with the GQDs suspensions ( $50\text{ mg L}^{-1}$ ) for 3 h. Bicarbonate buffer ( $50 \times 10^{-6}\text{ M}$ , pH 8.6) and  $H_2O_2$  ( $1 \times 10^{-6}\text{ M}$ ) were used as negative and positive control, respectively. Different letters stand for statistical differences between treatments at  $p < 0.05$  ( $n = 6$ ) as evaluated by one way ANOVA analysis.

the effects between the GQDs treatments, N-GQDs showed the lowest impacts while O-GQDs had the highest impact on the phytohormone contents.

## 2.9. ROS Generation and Oxidative Potential of GQDs

ROS can oxidize the XTT and form a substance having absorbance at 470 nm. As shown in **Figure 9**, the ROS generation by the GQDs under dark conditions was not significant as shown by that the absorbances are close to the baseline value (Figure 9A), while the ROS generation after exposure to light can be clearly seen (Figure 9B). The ability to generate ROS follows the order: O-GQDs > C-GQDs > N-GQDs. The possibility of GQDs reacting with antioxidants such as GSH in plants was examined. GSH oxidation capacity following the same order as ROS generation: O-GQDs > C-GQDs > N-GQDs. O-GQDs showed 0.26- and 4.09- fold higher GSH oxidation than C-GQDs and N-GQDs, respectively.

## 3. Discussion

GQDs have been extensively studied to explore their potential for use as drug delivery systems in humans.<sup>[10]</sup> The same principle may be applicable to plant systems, i.e., delivery of genes to a target position for improved photosynthesis via foliar spray.<sup>[11]</sup> However, unlike application as biomedicine, agricultural application requires large scale and high quantities which raises the concern as to whether the application could cause potential long term adverse effects on the agricultural ecosystem such as soil health as well as on animal and human health. This is especially important for root application of GQDs since this is the mostly studied scenario in the current literature. Their carbon-based nature endows GQDs with low potential toxicity to human as revealed by in vitro cellular and in vivo animal studies.<sup>[12]</sup> Unlike large graphene sheets, GQDs have a fast clearance rate in animals due to their ultrasmall size thus having low toxicity and high biocompatibility.<sup>[12]</sup> However,

the environmental application is a different case considering the enormous variance in the sensitivity of different species to chemicals including NMs with different toxic potential.<sup>[13]</sup> This may include not only the difference between animal and plants but also that the sensitivity of different plant species to GQDs may be different, which has been reported for many other NMs such as  $CeO_2$ <sup>[13]</sup> and  $ZnO$ .<sup>[14]</sup>

Our results demonstrated that GQDs had high toxicity to lettuce plants with no significant positive effects on the growth of hydroponic plant. The results are contradictory to those previously reported, which may be partially attributed to the difference sensitivity of plant species to GQDs. Indeed, high sensitivity of lettuce to NMs exposure has been reported previously.<sup>[15]</sup> For example,  $CeO_2$  NPs, which are generally considered to have low phytotoxicity, only inhibited the growth of lettuce with no effects on six other tested species.<sup>[16]</sup> The other reason for the inconsistency may be related to the discrepancy of the physicochemical properties of the GQDs. In our study, the sizes of the GQDs are between 5 and 8 nm, which are different from those used in previous studies.

Indeed, a study by Xu et al.<sup>[17]</sup> showed that only 10 nm GQDs showed positive effects on the growth of *Zephyranthes grandiflora* while other sizes, less than 10 nm (5 nm) or larger than 20 nm, had no positive effects. In fact, at the same concentration ( $400\text{ mg L}^{-1}$ ), 20 nm and 30 nm GQDs inhibited the plant growth. In addition to size, we focused on surface functionalization, which is another key factor that determines the fate and biological effects of graphene materials yet been not been studied as to whether it affects the interaction of GQDs with plants.

We used GQDs with three types of common functionalization, including amination, carboxylation and hydroxylation, each of which can be further functionalized (e.g., coupling, crosslinking, polymerization) for different application purposes. Our results exclusively showed that hydroxylation endows the GQDs with higher phytotoxicity than the other two functionalizations, with the lowest phytotoxicity arising from the aminated GQDs. Although there is no data in plant systems available for a comparison with our data, our results agree with some

previous studies using cell lines,<sup>[18]</sup> bacteria<sup>[19]</sup> and fish<sup>[20]</sup> that aminated graphene or GQDs usually have lower toxicity than carboxylated and hydroxylated ones. Our data showed that surface functionalization dependent toxicity was not only observed for phenotypical data such as seedling length and biomass, but also for physiological response including impairment of photosynthesis and triggering of antioxidant defence and phytohormone regulation.

Oxidative damage is a key mechanism of the toxicity induced by graphene-based materials.<sup>[21]</sup> GQDs, as small sized graphene, may share a similar mechanism. Indeed, the GQDs triggered oxidative responses as shown by the observed regulation of antioxidant enzymes and MDA over-accumulation in the lettuce plants (Figure 7). SOD and POD are two critical antioxidant enzymes defending against ambient stresses. The oxidative response to N-GQDs is not significant since only POD activity was upregulated at the 50 mg L<sup>-1</sup> exposure concentration. However, C-GQDs and O-GQDs triggered the upregulation of SOD activities even at 1 mg L<sup>-1</sup>, indicating the induction of plant defence following GQDs exposure. However, O-GQDs caused MDA accumulation in roots and shoots even at 1 mg L<sup>-1</sup>, suggesting that the plant failed to protect itself against the high oxidative damage. We further explored the mechanism inducing the oxidative damage from two aspects. We first examined whether GQDs can directly generate ROS that contributed to the oxidative damage. We found no significant ROS generated by GQDs under dark conditions which simulate the root soil environment (Figure 9A). However, light exposure triggered significant ROS generation with the following order: O-GQDs > C-GQDs > N-GQDs (Figure 9B). This suggests that ROS may be generated by GQDs that were translocated to leaves because plant leaves were exposed to light for 2/3 of the experimental period. This may also explain the higher sensitivity of leaves than roots to the GQDs. In addition, we examined another possibility, i.e., that GQDs may react with inherent plant antioxidants such as GSH thereby causing reduced antioxidant capacity. GSH is a non-enzymatic antioxidant that exists widely in living cells which can defend against oxidative damage by reacting with free radicals. Similar trends were found for GSH oxidation which followed the order: O-GQDs > C-GQDs > N-GQDs. This suggests that oxidation of antioxidants combining with direct ROS generation contributed to the GQDs induced toxicity and explained the discrepancy between the different surface functionalization.

One of the direct consequence of failure of the antioxidant system in plant leaves is the impairment of photosynthesis.<sup>[22]</sup> Photosynthesis in leaves generates large amount of ROS as by-products and thus require an efficient antioxidant network to maintain the ROS at low levels.<sup>[22]</sup> The high oxidative damage caused by C-GQDs and O-GQDs in leaves indicates over accumulation of ROS which resulted in a significant decrease of photosynthetic pigments (Figure 4). As a result, the accumulation of organic nutrients (carbohydrates), which are produced by the photosynthesis process, was inhibited (Figure 6).

The GQDs also induced imbalance of the mineral homeostasis in lettuce plants, which could be another mechanism causing the observed growth inhibition (Figure 5). Higher plants require at least 14 mineral elements to support their growth and reproduction.<sup>[23]</sup> Deprivation, deficiency or overload

of even one of the elements can cause growth impairment and physiological disorders such as chlorosis or necrosis. Our results showed that all the GQDs tested affect the balance of the mineral elements levels. N-GQDs treatments only upregulated two microelements (Cu and Zn), which had little impacts on plant growth. In fact, Cu and Zn are essential micronutrients playing significant roles in photosynthetic process. Increase of the levels of the two elements might be beneficial to plant growth, which have been implied from in our results that the protein contents in leaves were increased by N-GQDs treatment (Figure 6A). However, C-GQDs and O-GQDs caused imbalance of more elements at both low and high concentrations. In addition to the alteration of macroelements such as Ca, K, and P, the Mg content in lettuce leaves was reduced by 12% and 22% with 1 and 50 mg L<sup>-1</sup> O-GQDs treatments. Mg is the central element of chlorophyll pigments and also acts as an activator of the enzymes that are responsible for the transport of sugars into the phloem and further to other parts of the plants.<sup>[24]</sup> The reduction of Mg levels can lead to impaired photosynthesis and failure of transportation of the sugar to where it is required. In addition, the Cu content was also significantly enhanced in plant leaves after the 50 mg L<sup>-1</sup> C-GQDs (by 9.84-fold) and O-GQDs (by 2.76-fold) treatments. Cu is the cofactor of many key metalloproteins and plays key roles in the electron transfer in the photosynthetic process.<sup>[25]</sup> However, Cu is also highly toxic; high contents of Cu in plants generates excessive ROS and directly impairs the photosynthetic electron transport. Therefore, the high Cu contents in plant leaves induced by the C-GQDs and O-GQDs treatments may also contribute to the impairment of photosynthesis and plant growth. Another element that was dramatically increased by C-GQDs and O-GQDs treatment was Fe. The iron overload caused by graphene oxide has been reported previously. It is suggested that graphene oxide induced acidification of culture medium enhanced the upward translocation of Fe.<sup>[26]</sup> In our study, 50 mg L<sup>-1</sup> C-GQDs treatment increased the Fe levels in roots and leaves by 2.51- and 1.74- fold, which correlated with the low pH (3.1–3.3) of the medium caused by the C-GQDs. O-GQDs did not change the pH of the medium and N-GQDs increased the pH to neutral, which resulted in no change of Fe content in the plants. This suggests that Fe overload may contribute to the toxicity induced by the C-GQDs.

Phytohormones are a group of signalling molecules that play vital roles in modulating plant growth under various environmental conditions.<sup>[27]</sup> Plants can adjust their phytohormone levels to cope with ambient stress such as that caused by NMs exposure.<sup>[28]</sup> Recent studies also showed that CuO and Cu<sub>3</sub>(PO<sub>4</sub>)<sub>2</sub> can protect soybean plants from sudden death syndrome by modulation of nutritional and phytohormone levels.<sup>[28b]</sup> CeO<sub>2</sub> NMs also showed alleviation of plant stress caused by nitrogen deficiency or excess by modulation of the antioxidant system and phytohormones.<sup>[28a]</sup> The phytohormones tested herein, including ABA, IAA, GA3, and ZR, were all regulated by C-GQDs and O-GQDs. ABA is a well-known “stress phytohormone.”<sup>[29]</sup> Dramatic elevation of ABA levels induced by C-GQDs and O-GQDs suggest a stress response of the plants to the GQDs exposure. IAA plays critical roles in the regulation of plant growth and development.<sup>[30]</sup> It is also involved in adaptive modulation of plant growth under stress

conditions. Reduction of the IAA levels in roots and shoots by C-GQDs and O-GQDs suggests a stress response in the plants that led to impaired plant growth.<sup>[30]</sup> GA3 is another plant growth hormone regulating germination, stem elongation, flowering and senescence. Recently, a role for GA3 as a stress indicator is increasingly evident.<sup>[31]</sup> C-GQDs and O-GQDs at 50 mg L<sup>-1</sup> reduced the GA3 levels in roots and shoots, suggesting a stress response in the plants. ZR belongs to the cytokinin family of hormones that regulate plant growth.<sup>[32]</sup> It is often considered as an antagonist of ABA. Indeed, the ZR3 decreased with the increase of ABA in response to GQDs exposure. The overall response in phytohormones caused by O-GQDs was higher than that by C-GQDs. N-GQDs caused no detectable response in phytohormone levels.

Although N-GQDs seem safe to plant growth, it is worth noting that studies in aquatic systems showed that N-GQDs caused persistent DNA damage in zebrafish compared to O-GQDs, which persisted even after the exposure was halted.<sup>[33]</sup> Similarly, hydroxylated graphene showed higher acute neurotoxicity on human neuroblastoma cells than carboxylated and aminated graphene; however, the study also showed that aminated graphene caused more persistent toxicity than the other two functionalization.<sup>[18]</sup> These results indicate that longer-term study may be necessary in the future. In addition, a recent study showed that 1–10 mg L<sup>-1</sup> GQDs caused persistent toxicity to the photosynthesis of green algae (*Chlorella vulgaris*) which play a vital role in maintaining the food web in aquatic systems.<sup>[34]</sup> GQDs at 25 mg L<sup>-1</sup> could also cause hypoactivity of zebrafish larvae as well as acute inflammatory response and transcriptomic alteration.<sup>[35]</sup> Therefore, terrestrial application of GQDs would need to also consider the impacts of those GQDs released via the runoff to the aquatic system.

In summary, this study for the first time elucidated the mechanism involved in the surface-functionalization dependent phytotoxicity of GQDs to lettuce plants. The oxidation of antioxidants in plants and light-triggered ROS generation were found to be the critical reason for GQDs induced phytotoxicity. N-GQDs was relatively non-toxic compared with C-GQDs and O-GQDs with O-GQDs being the most toxic. The C-GQDs and O-GQDs triggered an oxidative response as well as modulation of the phytohormones. The consequence of the toxicity includes impaired photosynthesis, failure of the antioxidant system, disruption of mineral homeostasis, destruction of organic nutrients and retardance of plant growth. Phytohormone modulation was found to be a new mechanism by which GQDs act on plants. The findings provide new insights into the interaction of GQDs with plants as previous studies considered GQDs as non-toxic and even candidates for use as plant growth enhancers. We argue here that such application should consider plant species as well as the surface functionalization of the GQDs which are found to be key factors affecting the plant response to GQDs. We also suggest considering growth stage for such application because plants at seedling stage respond more sensitively to GQDs than at the germination stage. It should be noted that this is a short-term study carried out in hydroponic condition. Impacts of GQDs on plants in realistic soil environment over longer exposure time could be different and the mechanisms (e.g., light induced ROS generation will not likely occur in soil) involved will be complicated by the soil

components and exposure duration, which requires further studies.

## 4. Experimental Section

**Chemicals and Seeds:** GQDs (1 mg mL<sup>-1</sup> water suspension) were purchased from ACS Materials (USA). The morphology and pristine size of GQDs were observed on transmission electron microscope (TEM, JEOL 2100). Hydrodynamic size and  $\zeta$  potential of GQDs (50 mg L<sup>-1</sup>) were measured using dynamic light scattering (DLS, Malvern, UK). Fluorescence of the GQDs (10 mg L<sup>-1</sup>) was examined by measuring the three-dimensional excitation and emission matrix (3DEEM) spectra on a Varian Cary Eclipse Fluorescence Spectrophotometer (Agilent, USA). Fourier transform infrared (FTIR) spectra were recorded on a Bruker Tensor 27 IR spectrometer equipped with a DTGS (deuterated triglycine sulfate pyroelectric) detector. Samples were ground with KBr into fine powders for measurement. Spectra were recorded in the 4000–400 cm<sup>-1</sup> range with a resolution of 4 cm<sup>-1</sup>.

**Seed Germination:** Head lettuce (*Lactuca sativa*) seeds with uniform size were selected and immersed in 10% sodium hypochlorite solution for 15 min followed by rinsing in deionized water to ensure surface sterility. GQDs water suspensions of concentrations 0.1, 1, 10, 50 and 100 mg L<sup>-1</sup> were prepared and dispersed in an ultrasonic bath for 30 min before exposure. A wide range of concentrations were chosen to ensure observation of relevant phototoxic response at high dose as well as possible positive effects at low dose. One piece of filter paper (Whatman) was placed in a 10 cm × 1.5 cm Petri dish and immersed in 5 mL of as-prepared GQDs suspensions or deionized water as the control group. Fourteen seeds were arrayed in each dish with an even distance between seeds. All Petri dishes were then sealed tightly with parafilm to avoid water loss during germination. The seeds were allowed to germinate under darkness at 25 °C in an artificial climate chamber. For each treatment, four replicates were set. The germination was halted after 5 days. Germination rates were calculated and the root and shoot lengths were measured using a meter ruler.

**Ion Leakage:** In order to evaluate the cell membrane damage caused by GQDs exposure, ion leakage from the root cells was determined by measuring the conductivity of ions released from the roots.<sup>[36]</sup> In brief, the conductivity of deionized water was firstly measured ( $C_w$ ) using a Mettler Toledo conductivity probe (US). After 3 washes with deionized water to remove external contamination, the roots were immersed in 15 mL centrifuge tubes containing 3 mL deionized water. All samples were incubated in a temperature-controlled shaker (25 °C) at 150 rpm for 1 h. The roots were removed, and the electrolyte conductivity of the solution was measured ( $C_0$ ). After the measurement, samples were boiled for 15 min then cooled to room temperature, and the electrolyte conductivity ( $C_t$ ) was measured again. The electrolyte leakage (EL) ratio was calculated as: EL ratio =  $(C_t - C_w) / (C_0 - C_w)$ . Six replicate samples were tested for each data point. All the experiments were repeated three times.

**ROS Accumulation in Roots:** The ROS accumulation in roots after 5 days of germination was determined by DCFH-DA (2',7'-Dichlorodihydrofluorescein diacetate) staining. DCFH-DA can enter the cell and be oxidized by ROS, forming the green-fluorescent 2'-7'-dichlorofluorescein (DCF). In brief, the roots were thoroughly rinsed with deionized water and immersed in  $10 \times 10^{-6}$  M DCFH-DA solution in phosphate-buffered saline (PBS) buffer for 20 min. The roots were rinsed with deionized water again followed by blotting on tissue paper. The roots were then placed on microscope slides for observation using confocal microscopy using 515/30 nm band pass filter (Nikon ATR, Japan).

**Seedling Culture and Exposure:** Lettuce seeds were germinated in the dark for 5 days after being sterilized in 10% NaClO for 10 min. Uniform seedlings were selected and each seedling was anchored in plastic foam and transferred to a glass beaker containing modified ¼ strength Hoagland nutrient solution. All beakers were wrapped with

black plastic bags to simulate the dark environment in soil. Seedlings were then allowed to grow in an artificial growth chamber with a day/night temperature of 28/20 °C, day/night humidity of 50/70%, and a 14 h photoperiod for 10 days before treatment. GQD suspensions (0.1, 1, 10, 50 mg L<sup>-1</sup>) were prepared in freshly prepared nutrient solution followed by ultrasonic pre-treatment for 20 min. The seedlings were then exposed to the GQD suspensions for 2 weeks.

**Biomass Production and Inorganic Nutrients:** The plants were harvested after 2 weeks of exposure. Roots were rinsed with deionized water repeatedly. Roots and shoots were then separated, and the fresh weights were measured immediately after blotting with clean tissues. Dry weights were also measured after lyophilization. Leaf moisture was calculated as the weight loss after drying. To analyse the inorganic nutrients, dry roots and shoots were ground into fine powders and digested with a mixture of HNO<sub>3</sub> and H<sub>2</sub>O<sub>2</sub> (v/v: 3:1) on a heating plate (80 °C for 1 h, 120 °C for 3 h, and 160 °C for 0.5 h). The concentrations of elements including Fe, Mn, Cu, Zn, Ca, K, Mg, and P were measured by inductively coupled plasma optical emission spectroscopy (ICP-OES, Perkin Elmer, UK). Multielement standard solutions (0.5–50 mg L<sup>-1</sup>) containing all of the tested elements were used as external calibration. Blanks were analysed between every six samples. Certified reference material (GBW 07602 Bush Branches and Leaves) was digested, and spiking recovery experiments were performed for analytical method validation. Limits of detection and recoveries of the elements are reported in Table S1 in the Supporting Information.

**Organic Nutrient Content:** Accumulation of organic nutrients including protein, soluble sugar, starch and crude fibre in the lettuce plants were measured. In brief, soluble protein content was measured using a BCA protein assay kit (Thermo Fisher, US). Bovine serum albumin solutions with known concentrations (25–2000 µg mL<sup>-1</sup>) were prepared as standards for calibration. Six replicate samples were tested for each data point and the experiments were repeated three times. For total soluble sugar, reducing sugar and starch, 0.05g dry samples were homogenized in 80% ethanol and centrifuged at 2000 rpm for 20 min, the supernatant was used for analysis of sugar and starch content by measuring the absorbance at 490, 515, and 490 nm, respectively. Crude fibres were measured by igniting the dry residue after digestion of the dry samples with 1.25% NaOH and 1.25% H<sub>2</sub>SO<sub>4</sub>.<sup>[37]</sup> The crude fiber content was calculated as the loss of weight accounting for the weight of the digested samples. Full details of sugar and starch content measurements are provided in the SI.

**Chlorophyll Pigments:** The chlorophyll pigments in leaves were determined according to a previously described method.<sup>[38]</sup> In brief, fresh leaf samples were ground in liquid nitrogen and washed with 80% acetone until the sample color changed to white. The solution was passed through filter paper (Whatman) and the filtrates were diluted to a total volume of 10 mL. The absorbance at 663 nm, 645 nm and 470 nm were recorded, respectively. The contents of chlorophyll a and b and carotenoid were then calculated according to the equations in Figure S1 in the Supporting Information. Six replicate samples were tested for each data point. All the experiments were repeated three times.

**Antioxidant Enzyme Activity and Lipid Peroxidation:** Fresh roots and shoots were excised, homogenized with cold PBS (50 × 10<sup>-6</sup> M, pH 7.8) in an ice bath, and centrifuged at 10000g at 4 °C for 10 min. The supernatants were used for analyses of superoxide dismutase (SOD) and peroxidase (POD) activities and malondialdehyde (MDA) content using assay kits purchased from Sigma Aldrich (UK) following the manufacturer's instructions. To ensure accuracy and linearity, standard SOD, POD and MDA with known concentrations (6 concentrations) were prepared and analyzed following the same procedure described in the kits for sample analysis. Six replicate samples were tested for each data point and the experiments were repeated three times.

**Phytohormones Contents:** The levels of phytohormones including gibberellin 3 (GA3), abscisic acid (ABA), zeatin riboside (ZR) and indole-3-acetic acid (IAA) were determined following the method described previously.<sup>[39]</sup> Briefly, fresh root and shoot samples were homogenized in methanol and centrifuged at 5000g for 10 min. The supernatants were used to measure the phytohormones using the enzyme-linked

immunosorbent assay (ELISA) following the manufacturer's instruction (Solarbio, Beijing, China). All the tests were repeated three times. Six replicate samples were analysed for each data point. GA3, ABA, ZR and IAA with known concentrations were analysed as standards following the same procedure described in the assay kits.

**Glutathione (GSH) Oxidation and Superoxide Radical Anion (O<sub>2</sub><sup>-</sup>) Production by GQDs:** GSH oxidation test was performed following a previously described method with slight modification.<sup>[40]</sup> In brief, GQDs were pre-incubated in deionized water for 3 h. 0.5 mL GQDs with concentrations of 10 mg L<sup>-1</sup> were added to 10 mL of 50 × 10<sup>-6</sup> M bicarbonate buffer (pH 8.6) in a 25 mL conical flask and agitated at 100 rpm for 3 h in the dark at room temperature allowing reaction. The amount of non-oxidized GSH was quantified spectrophotometrically using Ellman's reagent (5,5'-dithiobis-(2-nitrobenzoic acid), DTNB), which reacts with the thiol groups of GSH to yield 3-thio-6-nitrobenzoate (TNB). The obtained medium was filtered through 0.22-µm syringe filters (Merck Millipore, UK). Then, 900 µL of the filtrates were added to 1.57 mL Tris-HCl buffer (pH 8.3) that contained 30 µL of 100 × 10<sup>-6</sup> M DTNB. The amount of thiol remaining in the reaction medium was quantified by measuring the absorbance at 412 nm.

To measure the O<sub>2</sub><sup>-</sup>, the GQDs dispersions (10 mg L<sup>-1</sup>, 1 mL) were mixed with 1 mL of 0.4 × 10<sup>-6</sup> M 2,3-bis-(2-methoxy-4-nitro-5-sulphophenyl)-2H-tetrazolium-5-carboxanilide (XTT, >90%) prepared in PBS solution (pH 7.0), and reacted in the dark for 5 h, followed by centrifugation at 10 000g (10 min) and then filtered through a 0.22 µm syringe filter (Merck Millipore, UK) to remove the residues. 250 µL of the filtrates were added per well of a 96-well plate. Three replicates were prepared for each sample. TiO<sub>2</sub> (Degussa, P25, 50 mg L<sup>-1</sup>) dispersion was exposed to UV light as a positive control for this assay. The production of O<sub>2</sub><sup>-</sup> was evaluated by reduction of XTT to form water-soluble XTT-formazan which can be measured by absorption at 470 nm.<sup>[41]</sup>

**Statistical Analysis:** Data were expressed as mean ± standard deviation (SD) (n = 6). Statistical analysis was performed on IBM SPSS 19.0. One way ANOVA was used to evaluate the significance between data (multiway comparison such that differences between all groups were all compared). p < 0.05 was considered significantly different.

## Supporting Information

Supporting Information is available from the Wiley Online Library or from the author.

## Acknowledgements

This work has received funding from the European Union's Horizon 2020 research and innovation programme via NanoSolveIT Project under grant agreement No 814572.

## Conflict of Interest

The authors declare no conflict of interest.

## Data Availability Statement

Research data are not shared.

## Keywords

graphene quantum dots, oxidative damage, phytohormones, phytotoxicity, surface functionalization



Received: December 30, 2020

Revised: February 15, 2021

Published online:

- [1] a) G. V. Lowry, A. Avellan, L. M. Gilbertson, *Nat. Nanotechnol.* **2019**, *14*, 517; b) M. Kah, N. Tufenkji, J. C. White, *Nat. Nanotechnol.* **2019**, *14*, 532.
- [2] T. Hofmann, G. V. Lowry, S. Ghoshal, N. Tufenkji, D. Brambilla, J. R. Dutcher, L. M. Gilbertson, J. P. Giraldo, J. M. Kinsella, M. P. Landry, *Nat. Food* **2020**, *1*, 416.
- [3] J. P. Giraldo, H. Wu, G. M. Newkirk, S. Kruss, *Nat. Nanotechnol.* **2019**, *14*, 541.
- [4] S. Kabiri, F. Degryse, D. N. Tran, R. C. da Silva, M. J. McLaughlin, D. Losic, *ACS Appl. Mater. Interfaces* **2017**, *9*, 43325.
- [5] D. Chakravarty, M. B. Erande, D. J. Late, *J. Sci. Food Agri.* **2015**, *95*, 2772.
- [6] P. Tian, L. Tang, K. Teng, S. Lau, *Mater. Today Chem.* **2018**, *10*, 221.
- [7] a) P. M. Carrasco, I. García, L. Yate, R. T. Zaera, G. Cabañero, H. J. Grande, V. Ruiz, *Carbon* **2016**, *109*, 658; b) C. Wang, Y. Sun, J. Jin, Z. Xiong, D. Li, J. Yao, Y. Liu, *Anal. Methods* **2018**, *10*, 1163.
- [8] Y. Xu, Y. Lu, J. Li, R. Liu, X. Zhu, *Nanoscale* **2020**, *12*, 15045.
- [9] P. Feng, B. Geng, Z. Cheng, X. Liao, D. Pan, J. Huang, *Braz. J. Bot.* **2019**, *42*, 29.
- [10] D. Iannazzo, A. Pistone, M. Salamò, S. Galvagno, R. Romeo, S. V. Giofrè, C. Branca, G. Visalli, A. Di Pietro, *Int. J. Pharm.* **2017**, *518*, 185.
- [11] S. H. Schwartz, B. Hendrix, P. Hoffer, R. A. Sanders, W. Zheng, *BioRxiv* **2019**, 722595.
- [12] Y. Chong, Y. Ma, H. Shen, X. Tu, X. Zhou, J. Xu, J. Dai, S. Fan, Z. Zhang, *Biomaterials* **2014**, *35*, 5041.
- [13] P. Zhang, Y. Ma, C. Xie, Z. Guo, X. He, E. Valsami-Jones, I. Lynch, W. Luo, L. Zheng, Z. Zhang, *Environ. Sci.: Nano* **2019**, *6*, 60.
- [14] M. L. López-Moreno, G. de la Rosa, J. Á. Hernández-Viezas, H. Castillo-Michel, C. E. Botez, J. R. Peralta-Videa, J. L. Gardea-Torresdey, *Environ. Sci. Technol.* **2010**, *44*, 7315.
- [15] P. Zhang, Y. Ma, Z. Zhang, X. He, Y. Li, J. Zhang, L. Zheng, Y. Zhao, *Nanotoxicology* **2015**, *9*, 1.
- [16] Y. Ma, L. Kuang, X. He, W. Bai, Y. Ding, Z. Zhang, Y. Zhao, Z. Chai, *Chemosphere* **2010**, *78*, 273.
- [17] Y. Xu, Y. Lu, J. Li, R. Liu, X. J. N. Zhu, *Nanoscale* **2020**, *12*, 15045.
- [18] Z. Guo, P. Zhang, A. J. Chetwynd, H. Q. Xie, E. Valsami-Jones, B. Zhao, I. Lynch, *Nanoscale* **2020**, *12*, 18600.
- [19] C. Xie, P. Zhang, Z. Guo, X. Li, Q. Pang, K. Zheng, X. He, Y. Ma, Z. Zhang, I. Lynch, *Sci. Total Environ.* **2020**, *747*, 141546.
- [20] J. Hu, W. Lin, B. Lin, K. Wu, H. Fan, Y. Yu, *Ecotoxicol. Environ. Saf.* **2019**, *169*, 370.
- [21] L. Ou, B. Song, H. Liang, J. Liu, X. Feng, B. Deng, T. Sun, L. Shao, *Part. Fibre Toxicol.* **2016**, *13*, 57.
- [22] S. Khorobrykh, V. Havurinne, H. Mattila, E. Tyystjärvi, *Plants* **2020**, *9*, 91.
- [23] P. White, P. Brown, *Ann. Bot.* **2010**, *105*, 1073.
- [24] X. Ye, X.-F. Chen, C.-L. Deng, L.-T. Yang, N.-W. Lai, J.-X. Guo, L.-S. Chen, *Plants* **2019**, *8*, 389.
- [25] I. Yruela, *Braz. J. Plant Physiol.* **2005**, *17*, 145.
- [26] P. Zhang, Z. Guo, W. Luo, F. A. Monikh, C. Xie, E. Valsami-Jones, I. Lynch, Z. Zhang, *Environ. Sci. Technol.* **2020**, *54*, 3181.
- [27] S. H. Wani, V. Kumar, V. Shriram, S. K. Sah, *Crop J.* **2016**, *4*, 162.
- [28] a) Y. Wang, P. Zhang, M. Li, Z. Guo, S. Ullah, Y. Rui, I. Lynch, *Environ. Sci.: Nano* **2020**, *7*, 2930; b) C. Ma, J. Borgatta, B. G. Hudson, A. A. Tamijani, R. De La Torre-Roche, N. Zuverza-Mena, Y. Shen, W. Elmer, B. Xing, S. E. Mason, *Nat. Nanotechnol.* **2020**, *15*, 1033.
- [29] K. Vishwakarma, N. Upadhyay, N. Kumar, G. Yadav, J. Singh, R. K. Mishra, V. Kumar, R. Verma, R. Upadhyay, M. Pandey, *Front. Plant Sci.* **2017**, *8*, 161.
- [30] A. Kohli, N. Sreenivasulu, P. Lakshmanan, P. P. Kumar, *Plant Cell Rep.* **2013**, *32*, 945.
- [31] E. H. Colebrook, S. G. Thomas, A. L. Phillips, P. Hedden, *J. Exp. Biol.* **2014**, *217*, 67.
- [32] V. Verma, P. Ravindran, P. P. Kumar, *BMC Plant Biol.* **2016**, *16*, 86.
- [33] J. Hu, W. Lin, B. Lin, K. Wu, H. Fan, Y. Yu, *Ecotoxicol. Environ. Saf.* **2019**, *169*, 370.
- [34] W. Kang, X. Li, A. Sun, F. Yu, X. Hu, *Environ. Sci. Technol.* **2019**, *53*, 3791.
- [35] Z. G. Wang, Z. Rong, D. Jiang, E. S. Jing, X. Qian, S. Jing, Y. P. Chen, Z. Xin, G. Lu, J. Z. Li, *Biomed. Environ. Sci.* **2015**, *28*, 341.
- [36] D. Cui, P. Zhang, Y. Ma, X. He, Y. Li, J. Zhang, Y. Zhao, Z. Zhang, *Environ. Sci.: Nano* **2014**, *1*, 459.
- [37] X. L. Chen, L. C. Wang, T. Li, Q. C. Yang, W. Z. Guo, *Sci. Rep.* **2019**, *9*, 6926.
- [38] H. K. Lichtenthaler, A. R. Wellburn, Portland Press Ltd., **1983**.
- [39] H. Gawronska, A. Deji, H. Sakakibara, T. Sugiyama, *Plant Physiol. Biochem.* **2003**, *41*, 605.
- [40] F. Perreault, A. F. De Faria, S. Nejati, M. Elimelech, *ACS Nano* **2015**, *9*, 7226.
- [41] S. Liu, T. H. Zeng, M. Hofmann, E. Burcombe, J. Wei, R. Jiang, J. Kong, Y. Chen, *ACS Nano* **2011**, *5*, 6971.